Supplementary Material

Manipulating Peripheral Substituents of TADF Emitters based on Carbazole/Oxadiazole Hybrids to Achieve High-efficiency OLEDs

Die Hu,[a] Mengyuan Zhu,[a] Changsheng Shi,[b]* Wenbo Yuan,[a] Ning Sun,[b,]* Bin Huang,[c,]* and Youtian Tao[a,]*

[a] Key Laboratory of Flexible Electronics & Institute of Advanced Materials, Nanjing Tech University, Nanjing, P. R. China. E-mail address: iamyttao@njtech.edu.cn

[b] Department of Physics, Center for Optoelectronics Engineering Research, Yunnan University, Kunming 650091, China. E-mail address: csshi@ynu.edu.cn; ning.sun@ynu.edu.cn

[c] College of Life Sciences and Chemistry, Jiangsu Key Laboratory of Biofunctional Molecule, Jiangsu Second Normal University, Nanjing, P. R. China. E-mail address: huangbinhb31@sina.com

Experimental section

Materials

All the reagents were purchased from Energy Chemical Co. and Sinopharm Chemical Reagent Co. without further purification. All the solvents were used as received from Nanjing WANQING chemical Glass ware & Instrument Co. and J&K Scientific.

General procedures

^{1}H NMR spectra were recorded on a Bruker DMX-500 spectrometer in deuterochloroform using tetramethylsilane (TMS; δ = 0 ppm) as an internal standard. Mass spectra were recorded using a Bruker Autoflex matrix assisted laser desorption/ionization time-of-flight (MALDI-TOF). Elemental analyses (EA) of C, H, N, and S were performed on a Vario EL III microanalyzer. Absorption spectra: Ultraviolet-visible (UV-Vis) absorption spectra of solution in dichloromethane and thin film on a quartz substrate were measured using Shimadzu UV-2500 recording spectrophotometer, and the photoluminescence (PL) spectra were recorded using a Hitachi F-4600 fluorescence spectrophotometer. Thermal gravimetric analysis (TGA) was undertaken with a METTLER TOLEDO TGA2 instrument. The thermal stability of the samples was determined by measuring their weight loss at a heating rate of 10^{o}C min^{-1} from 25 to 500^{o}C using 3 mg sample under a nitrogen atmosphere. Cyclic voltametry (CV): The electrochemical cyclic voltammetry was conducted on a CHI voltammetric analyzer, in a 0.1 mol L^{-1} acetonitrile solution of tetrabutylammonium hexafluorophosphate (n-Bu_4NPF_6) at a potential scan rate of 100 mV s^{-1}. The conventional three electrode configuration consists of a platinum working electrode, a platinum wire counter electrode, and an Ag/AgCl wire pseudo-reference electrode. The polymer sample was coated on the platinum sheet of working electrode. The reference electrode was checked versus ferrocenium-ferrocene (Fc^+/Fc) as internal standard as recommended by IUPAC (the vacuum energy level: 24.8 eV). All the solutions were deaerated by bubbling nitrogen gas for a few minutes prior to the electrochemical measurements. HOMO energy levels were calculated from the equation of E_{HOMO} = - (E_{onset} (ox) + 4.8) eV, and LUMO energy levels were deduced from the optical band gap (E_g) values and HOMO levels.

OLED fabrication and measurements

The electroluminescent devices were fabricated by vacuum deposition technology, and all

functional layers were fabricated on pre-treated indium tin oxide (ITO) substrates. ITO glass substrates were successively cleaned by ultrasonic wave with detergent, alcohol, acetone and deionized water, then dried at 120°C in a vacuum oven for more than 60 min. The structure of the TADF device was ITO/HAT-CN (3 nm)/TAPC (45 nm)/EML (20 nm)/TmPyPB (40 nm)/Liq (1 nm)/Al (100 nm). Firstly, 3 nm of 1,4,5,8,9,11-hexaazatriphenylenehexacarbonitrile (HAT-CN) was deposited on ITO substrates as hole injection layer, followed by 45 nm of 4,4'-cyclohexylidenebis[*N*,*N*-bis(4-methylphenyl)aniline] (TAPC) used as hole transport layer. 20 nm of emitting layer containing 2,5-bis(2-(9*H*-carbazol-9-yl)phenyl)-1,3,4-oxadiazole (*o*-CzOXD) or (2,6-Bis[3-(carbazol-9-yl)phenyl]pyridine)(26DCzPPy) host doped with emitters was deposited on the films mentioned above. Finally, the electron transport layer was 1,3,5-tri(m-pyrid-3-ylphenyl)benzene (TmPyPB) for 40 nm, meanwhile, the 1 nm of Liq and hundred-nanometer of Al were considered as the cathode layers. Current density-voltage-luminance (*J*-*V*-*L*) characteristics were tested through using a Keithley source measurement unit (Keithley 2400 and Keithley 2000) and a calibrated silicon photodiode. In addition, the EL spectra were measured by a Spectrascan PR650 spectrophotometer. It should be noted that the measurements were carried out at room temperature under ambient condition.

Computational details

The ground-state geometries were optimized with Gaussian 09 program package using the B3LYP (Becke three parameters hybrid functional with Lee-Yang-Perdew correlation) functional and 6-31G(d) basis set.[1-2] The highest occupied and lowest unoccupied natural transition orbitals (HONTO and LUNTO) of T_1 and S_1 were both simulated at the wB97XD/6-311G(d,p) level. 3-D structure and molecular orbitals were visualized using Gauss view.

Analyses of rate constants

The rate constants were analyzed according to the literature method with the assumption that $k_{RISC} >> k_r^T + k_{nr}^T$, i.e. almost complete harvesting of triplet excitons to singlets. The rate constant of fluorescent radiative decay from S_1 to S_0 states (k_F), the rate constant of the ISC, the rate constant of RISC, the rate constant of IC and the rate constant of triplet non-radiative decay (k_{nr}^T) can be obtained:[3-4]

$$k_F = \frac{\Phi_P}{\tau_P} \qquad (1)$$

$$\Phi_{ISC} = 1 - \Phi_P \qquad (2)$$

$$\Phi_P = \frac{k_F}{k_F + k_{ISC}} \qquad (3)$$

$$k_{RISC} = \frac{k_P k_d \Phi_d}{k_{ISC} \Phi_P} \qquad (4)$$

$$\Phi = \frac{k_F}{k_F + k_{IC}} \qquad (5)$$

$$k_{nr}{}^T = k_d - (1 - \frac{k_{ISC}}{k_F + k_{ISC}}) k_{RISC} \qquad (6)$$

Where k_p and k_d represent the decay rate constant of prompt and delayed fluorescence ($k_P = \frac{1}{\tau_P}$, $k_d = \frac{1}{\tau_d}$), respectively. Φ_P and Φ_d represent quantum yields for the prompt and

delayed fluorescence components. All the above parameters can be experimentally determined from typical and transient PL characteristics.

Synthesis of compounds

1. The synthetic routes of 5FOXD, *m*$CF_3$5FOXD, *p*$CF_3$5FOXD and d$CF_3$5FOXD.

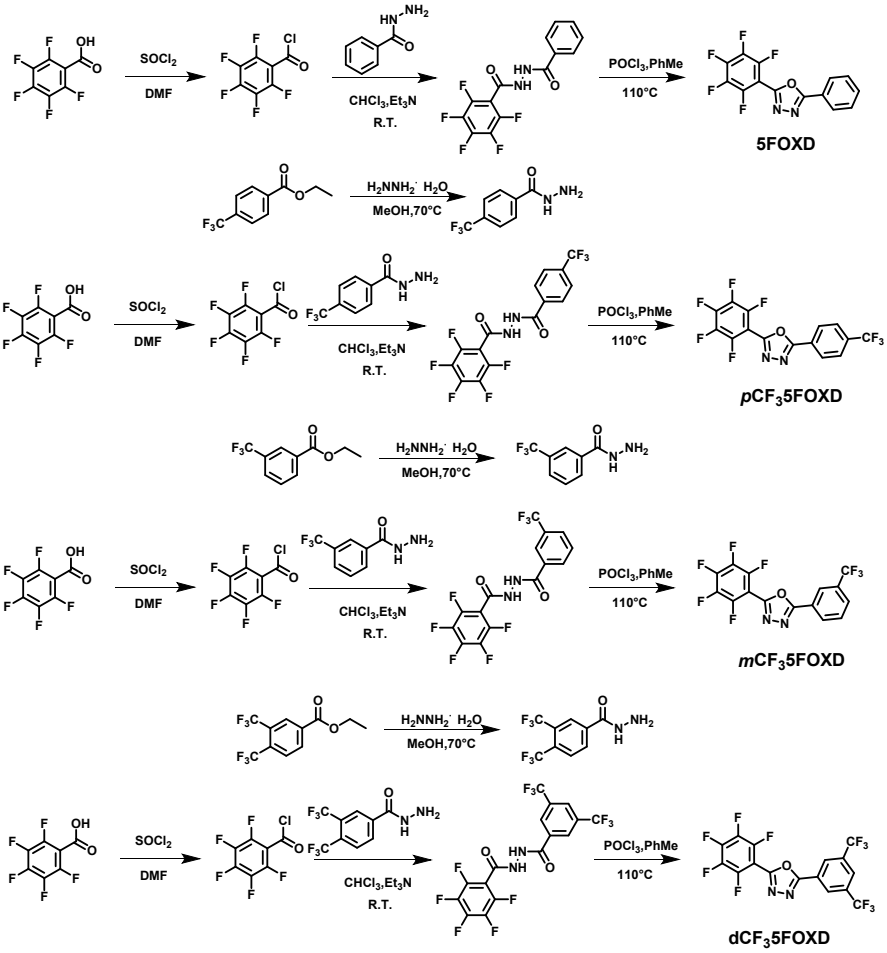

Scheme S1. The synthetic routes of 5FOXD, *m*$CF_3$5FOXD, *p*$CF_3$5FOXD and d$CF_3$5FOXD.

2. The synthetic route of 5CzOXD.

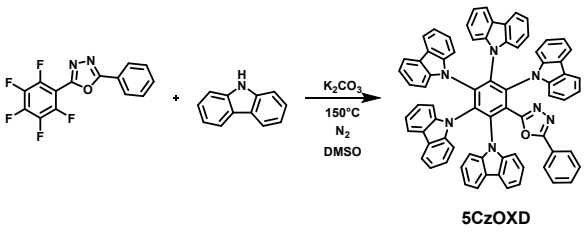

Scheme S2. The synthetic route of 5CzOXD.

A mixture of 5FOXD (0.5 g, 1.6 mmol),9*H*-carbazole (1.61 g, 9.61 mmol) and K_2CO_3 (3.98 g, 28.83 mmol) in dimethyl sulfoxide (DMSO) (30 mL) was stirred at 150°C for 24 h under an N_2 atmosphere. After cooling to room temperature, the mixture was poured into water, filtered, and then purified by column chromatography over silica gel with dichloromethane/petroleum ether as the eluent to afford a green solid (Yield: 80%). ^{1}H-NMR (400 MHz, $CDCl_3$) δ ppm: 7.62-7.60 (m, 4H), 7.36 (d, *J* = 8 Hz, 4H), 7.29 (t, *J* = 12 Hz, 3H), 7.24 (s, 3H), 7.22-7.19 (m, 7H), 7.07 (t, *J* = 16 Hz, 2H), 6.94 (t, *J* = 12 Hz, 8H), 6.79-6.72 (m, 8H), 6.68-6.58 (m, 6H). ^{13}C-NMR (100 MHz,

$CDCl_3$) δ ppm: 164.04, 157.61, 139.68, 138.06, 137.15, 126.53, 123.89, 120.43, 119.43, 110.82, 110.59, 109.48. MALDI-TOF (m/z): calcd. for $C_{74}H_{45}N_7O$: 1047.37; found: 1047.48. Anal. calcd. for $C_{74}H_{45}N_7O$: C 84.79, H 4.33, N 9.35%; found: C 85.17, H 4.12, N 9.29%.

3. The synthetic route of 5tCzOXD.

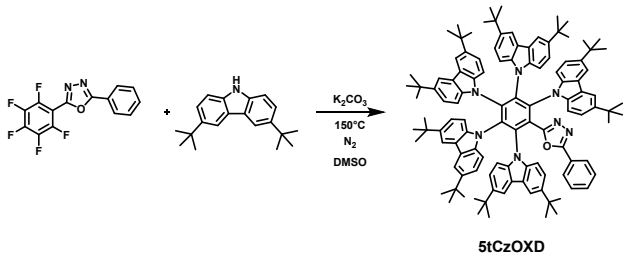

Scheme S3. The synthetic route of 5tCzOXD.

A mixture of 5FOXD (0.5 g, 1.6 mmol), 3,6-di-*tert*-butyl-9*H*-carbazole (2.69 g, 9.61 mmol) and K_2CO_3 (3.98 g, 28.83 mmol) in dimethyl sulfoxide (DMSO) (30 mL) was stirred at 150°C for 24 h under an N_2 atmosphere. After cooling to room temperature, the mixture was poured into water, filtered, and then purified by column chromatography over silica gel with dichloromethane/petroleum ether as the eluent to afford a green solid (Yield: 80%). ^{1}H-NMR (400 MHz, $CDCl_3$) δ ppm: 7.49 (d, *J* = 1.6 Hz, 4H), 7.27 (d, *J* = 12 Hz, 5H), 7.22 (d, *J* = 4 Hz, 2H), 7.09 (t, *J* = 16 Hz, 2H), 6.95-6.90 (m, 14H), 6.83 (d, *J* = 8 Hz, 2H), 6.62-6.57 (m, 6H), 1.20 (t, *J* = 4 Hz, 90H). ^{13}C-NMR (100 MHz, $CDCl_3$) δ ppm: 142.83, 142.68, 142.62, 137.14, 128.11, 123.07, 122.18, 115.01, 110.28, 110.18, 109.12, 34.48, 34.35, 31.89, 31.86. MALDI-TOF (m/z): calcd. for $C_{114}H_{125}N_7O$: 1607.99; found: 1608.0. Anal. calcd. for $C_{114}H_{125}N_7O$: C 85.08, H 7.83, N 6.09%; found: C 85.36, H 7.72, N 5.99%.

4. The synthetic route of *m*$CF_3$5tCzOXD.

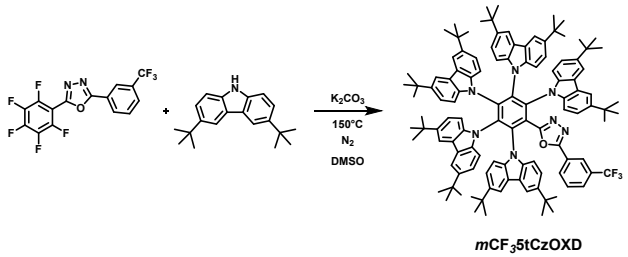

Scheme S4. The synthetic route of *m*$CF_3$5tCzOXD.

The synthetic process of *m*$CF_3$5tCzOXD was similar to that for 5tCzOXD as green powder with a yield of 81%. ^{1}H-NMR (400 MHz, $CDCl_3$) δ ppm: 7.54 (d, *J* = 4 Hz, 4H), 7.29 (d, *J* = 12 Hz, 5H), 7.23 (d, *J* = 2 Hz, 2H), 7.17 (s, 1H), 7.03-6.89 (m, 16H), 1.20 (d, *J* = 2.8 Hz, 90H). ^{13}C-NMR (100 MHz, $CDCl_3$) δ ppm: 142.97, 142.76, 142.70, 137.15, 124.31, 123.14, 122.19, 115.02, 110.24, 110.17,

109.01, 34.46, 34.35, 31.85, 31.82. MALDI-TOF (m/z): [M^+] calcd. for $C_{115}H_{124}F_3N_7O$: 1677.3; found: 1676.0. Anal. calcd. for $C_{115}H_{124}F_3N_7O$: C 82.35, H 7.45, N 5.85%; found: C 81.86, H 7.37, N 5.78%.

5. The synthetic route of *p*$CF_3$5tCzOXD.

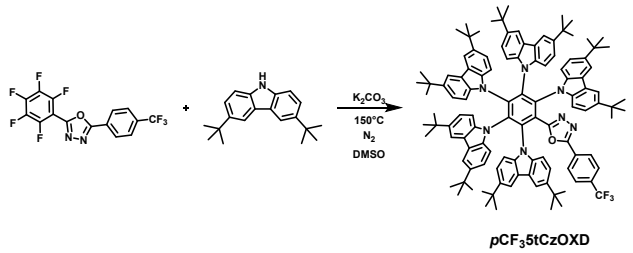

Scheme S5. The synthetic route of *p*$CF_3$5tCzOXD.

The synthetic process of *p*$CF_3$5tCzOXD was similar to that for 5tCzOXD as green powder with a yield of 85%. ^{1}H-NMR (400 MHz, $CDCl_3$) δ ppm: 7.50 (d, *J* = 2 Hz, 4H), 7.36 (d, *J*=8 Hz, 2H), 7.25 (d, *J* = 1.6 Hz, 4H), 7.23 (d, *J* = 2 Hz, 2H), 6.96-6.90 (m, 16H), 6.63-6.58 (m, 6H), 1.20 (t, *J* = 5.6 Hz, 90H). ^{13}C-NMR (100 MHz, $CDCl_3$) δ ppm: 143.05, 142.81, 142.75, 137.12, 124.35, 123.15, 122.24, 115.08, 110.16, 109.11, 34.51, 34.38, 31.88. MALDI-TOF (m/z): [M^+] calcd. for $C_{115}H_{124}F_3N_7O$: 1677.3; found: 1676.0. Anal. calcd. for $C_{115}H_{124}F_3N_7O$: C 82.35, H 7.45, N 5.85%; found: C 82.72, H 7.52, N 5.82%.

6. The synthetic route of d$CF_3$5CzOXD.

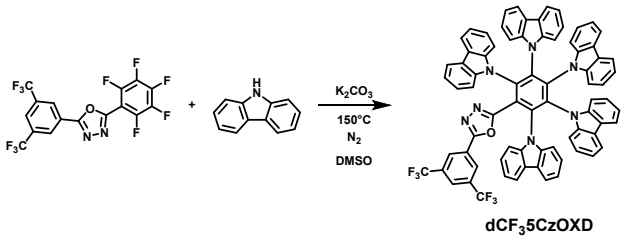

Scheme S6. The synthetic route of d$CF_3$5CzOXD.

The synthetic process of d$CF_3$5CzOXD was similar to that for 5CzOXD as green powder with a yield of 86%. ^{1}H-NMR (400 MHz, $CDCl_3$) δ ppm: 7.78 (s, 1H), 7.65-7.63 (m, 4H), 7.37 (d, *J* = 8 Hz, 4H), 7.31 (d, *J* = 8 Hz, 2H), 7.24-7.19 (m, *J*=20 Hz, 13H), 6.97-6.95 (m, 7H), 6.80-6.73 (m, 6H), 6.69-6.59 (m, 6H). ^{13}C-NMR (100 MHz, $CDCl_3$) δ ppm: 161.55, 158.71, 138.18, 137.91, 137.75, 137.11, 131.99, 120.76, 119.47, 110.60, 110.35, 109.15. MALDI-TOF (m/z): [M^+] calcd. for $C_{76}H_{43}F_6N_7O$: 1183.34; found: 1181.22. Anal. calcd. for $C_{76}H_{43}F_6N_7O$: C 77.08, H 3.93, N 8.28%; found: C 77.14, H 3.48, N 8.19%.

7. The synthetic route of $dCF_3$5tCzOXD.

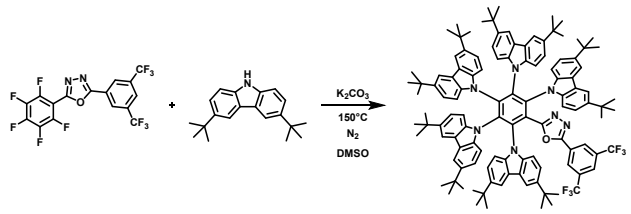

$dCF_3$5tCzOXD

Scheme S7. The synthetic route of $dCF_3$5tCzOXD.

The synthetic process of $dCF_3$5tCzOXD was similar to that for 5tCzOXD as green powder with a yield of 81%.^{1}H-NMR (400 MHz, $CDCl_3$) δ ppm: 8.05 (d, *J* = 1.6 Hz, 1H), 7.75 (s, 1H), 7.57 (d, *J* = 1.6 Hz, 4H), 7.45-7.43 (m, 1H), 7.34 (s, 2H), 7.32 (d, *J* = 8 Hz, 1H), 7.23-7.22 (m, 4H), 6.96-6.86 (m, 14H), 6.61-6.57 (m, 5H), 1.19 (t, *J* = 7.2 Hz, 90H). ^{13}C-NMR (100 MHz, $CDCl_3$) δ ppm: 143.09, 142.84, 142.76, 137.15, 132.24, 131.91, 123.86, 122.19, 115.02, 110.19, 110.14, 109.06, 108.85, 34.45, 34.35,31.84, 31.74. MALDI-TOF (m/z): calcd. for $C_{116}H_{123}F_6N_7O$: 1744.0; found: 1744.0. Anal. calcd. for $C_{116}H_{123}F_6N_7O$: C 79.83, H 7.10, N 5.46%; found: C 79.83, H 6.91, N 5.40%.

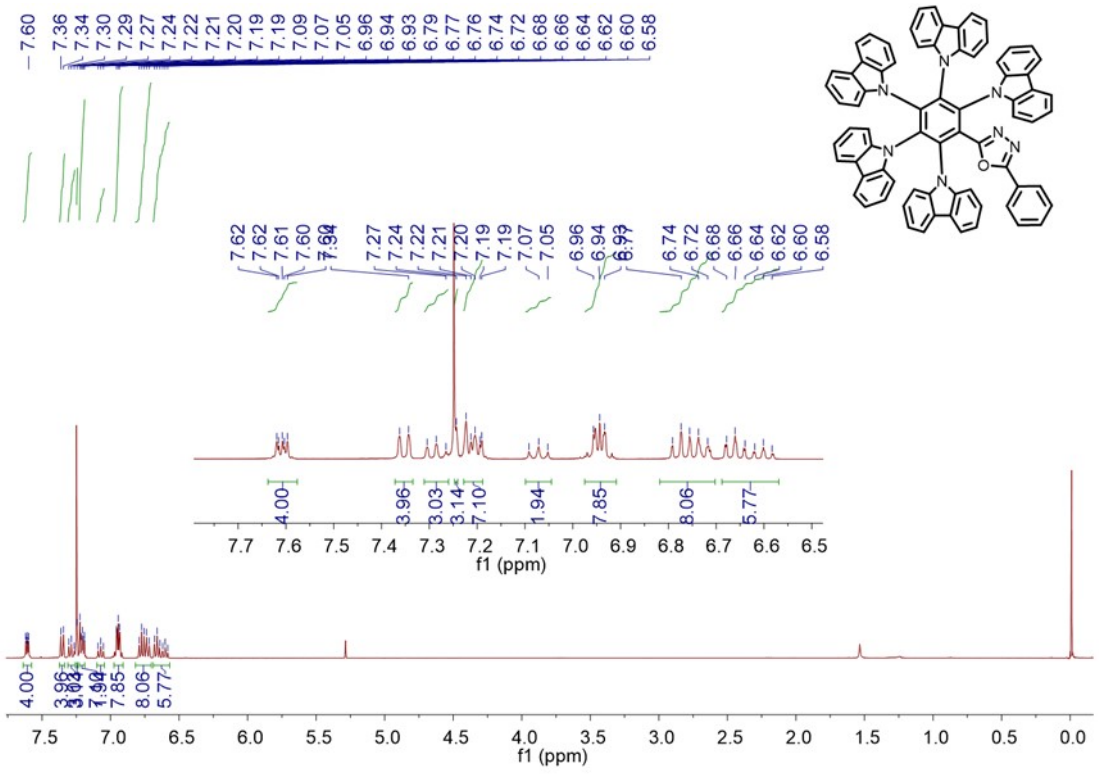

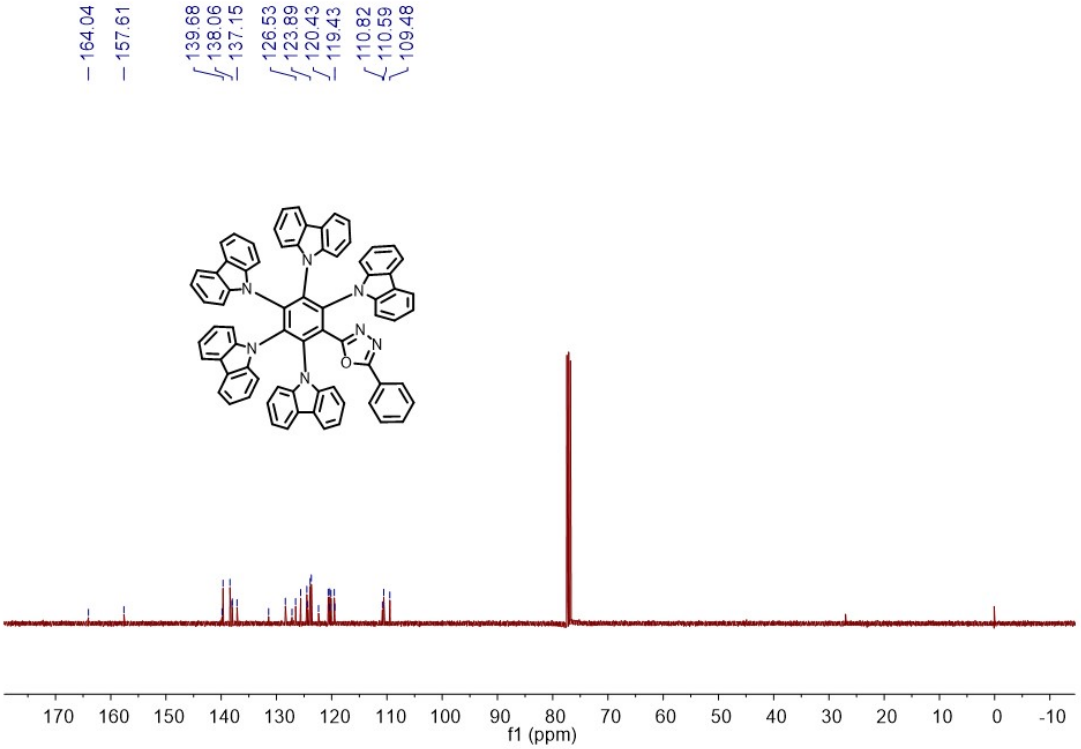

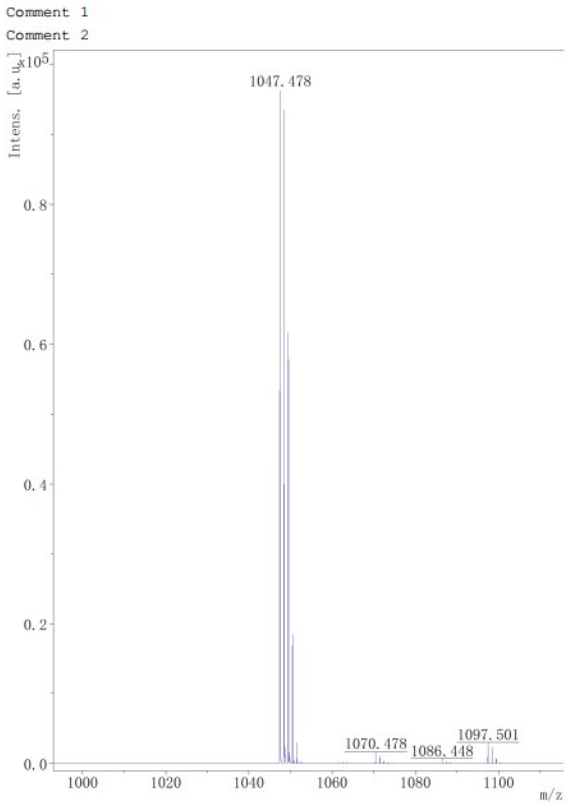

Fig. S1. ^{1}H NMR spectra, ^{13}C NMR spectra and mass spectrometry of the target compound 5CzOXD.

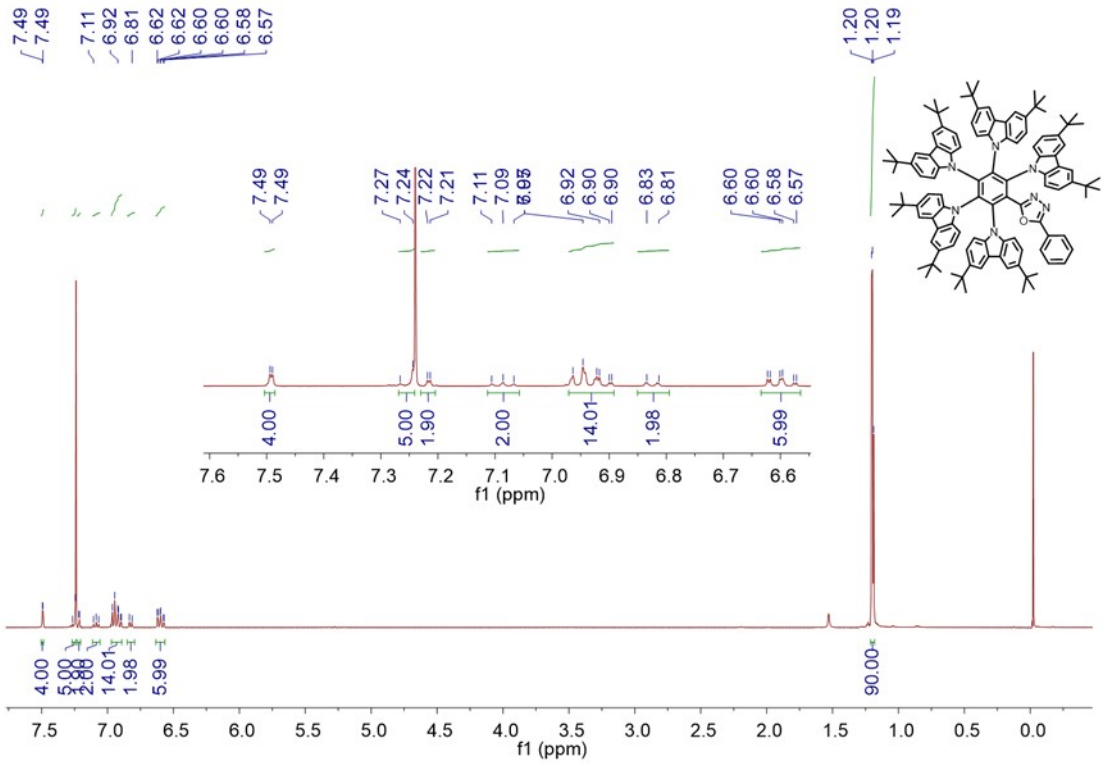
7.49
7.49
7.11
6.92
6.81
6.62
6.62
6.60
6.60
6.58
6.57
1.20
1.20
1.19
4.00
5.00
1.90
2.00
14.01
1.98
5.99
90.00
f1 (ppm)

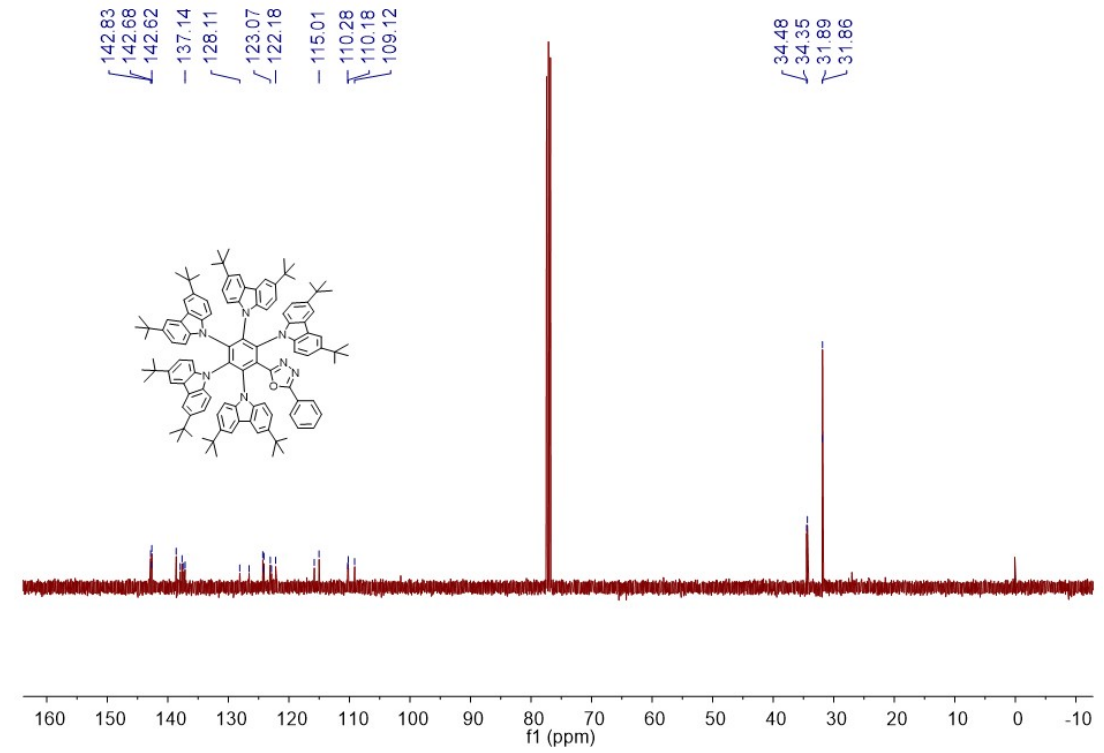
142.83
142.68
142.62
137.14
128.11
123.07
122.18
115.01
110.28
110.18
109.12
34.48
34.35
31.89
31.86
f1 (ppm)

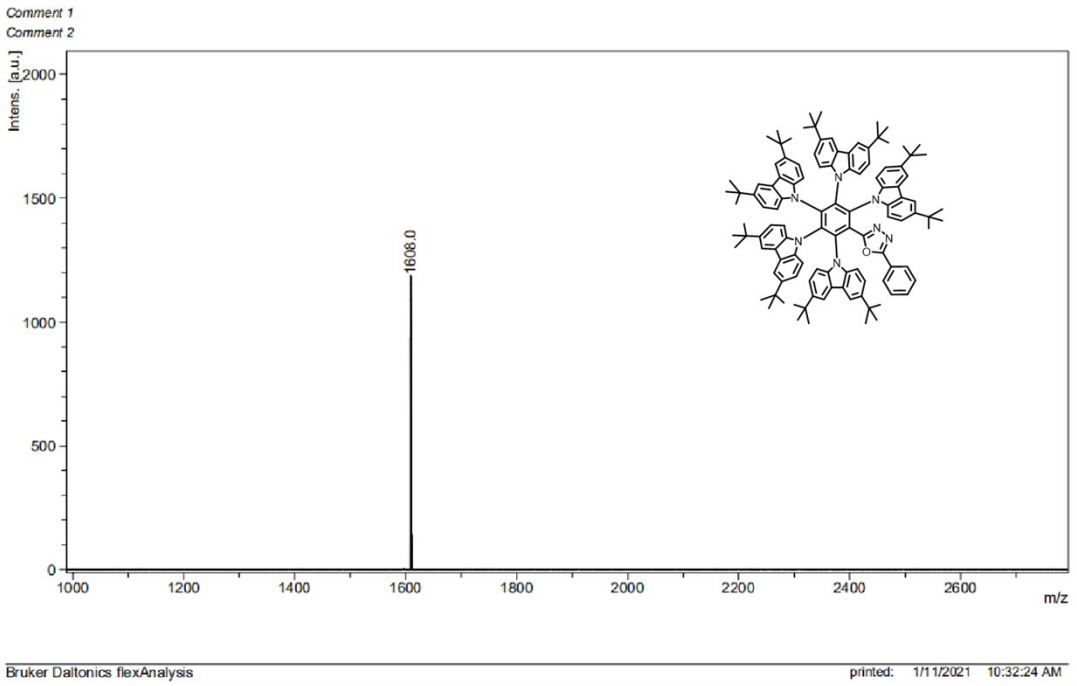

Fig. S2. ^{1}H NMR spectra, ^{13}C NMR spectra and mass spectrometry of the target compound 5tCzOXD.

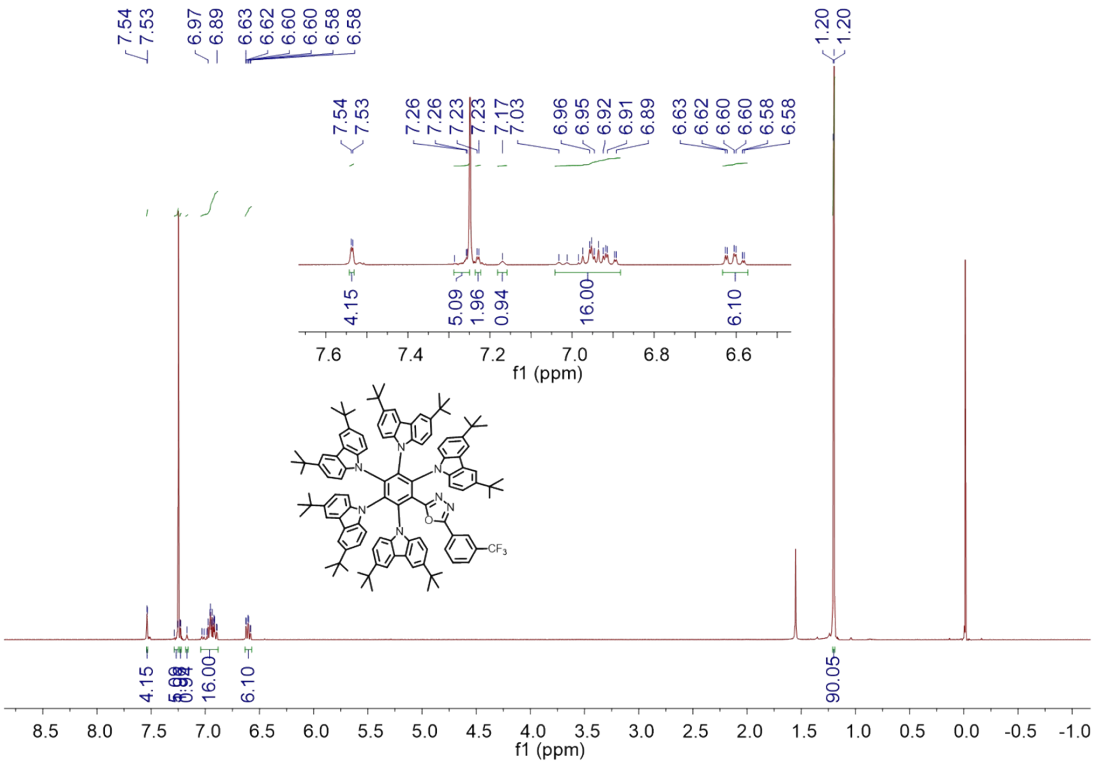

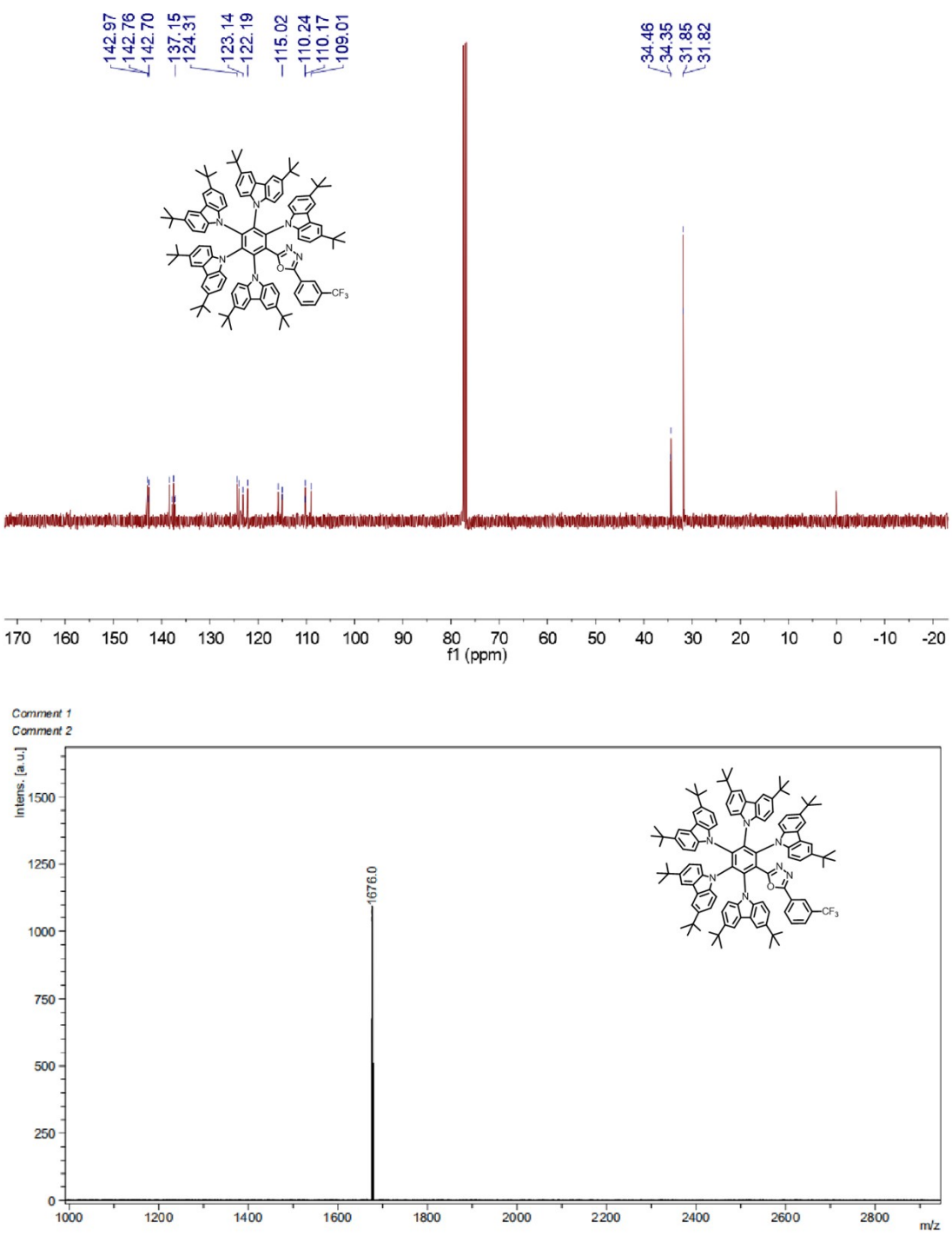

Fig. S3. ^{1}H NMR spectra, ^{13}C NMR spectra and mass spectrometry of the target compound *m*$CF_3$5tCzOXD.

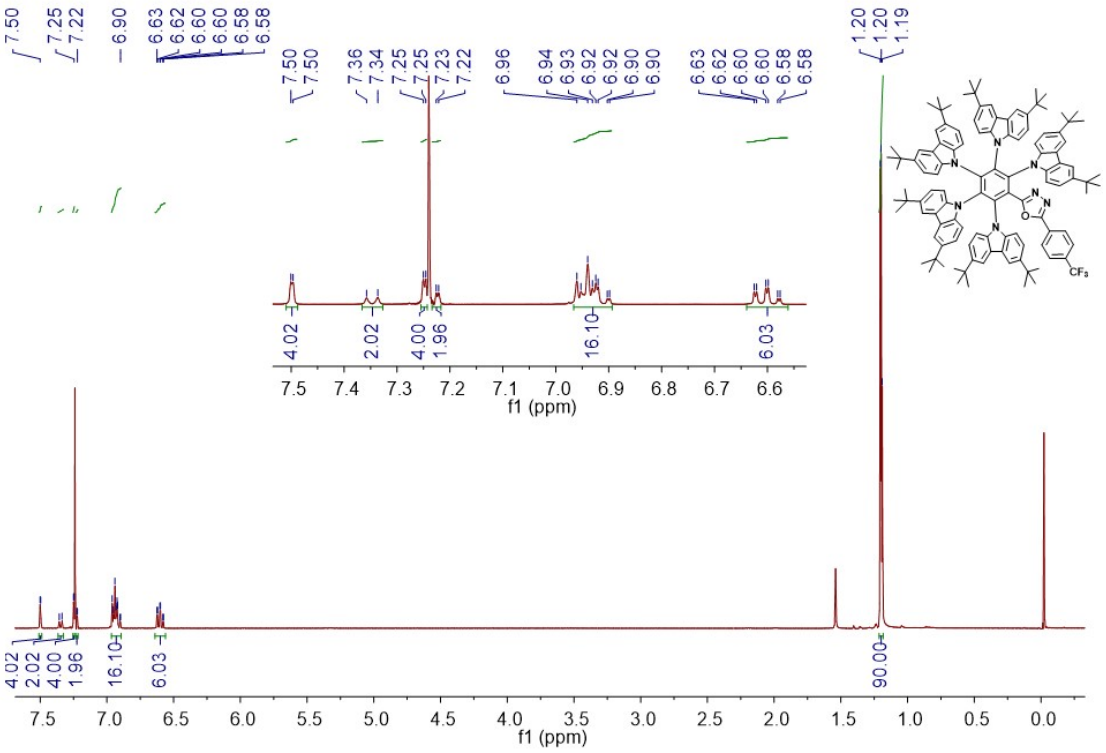
7.50
7.25
7.22
6.90
6.63
6.62
6.60
6.60
6.58
6.58
1.20
1.20
1.19
4.02
2.02
4.00
1.96
16.10
6.03
90.00
f1 (ppm)

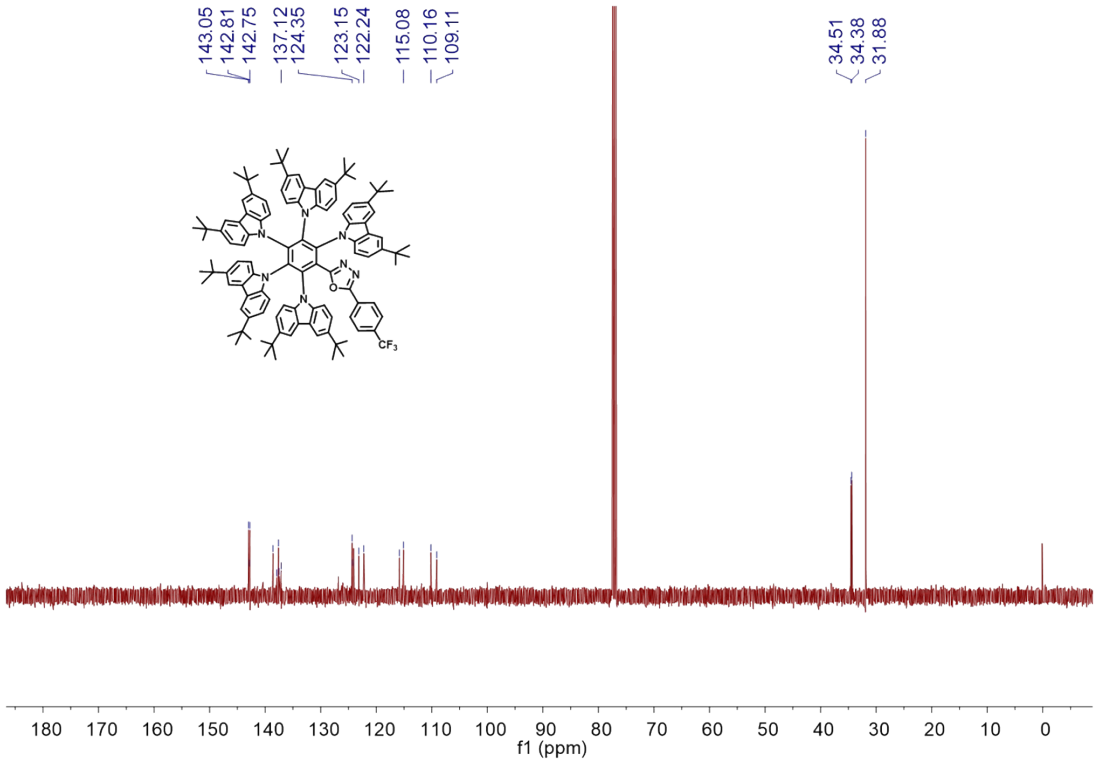
143.05
142.81
142.75
137.12
124.35
123.15
122.24
115.08
110.16
109.11
34.51
34.38
31.88
f1 (ppm)

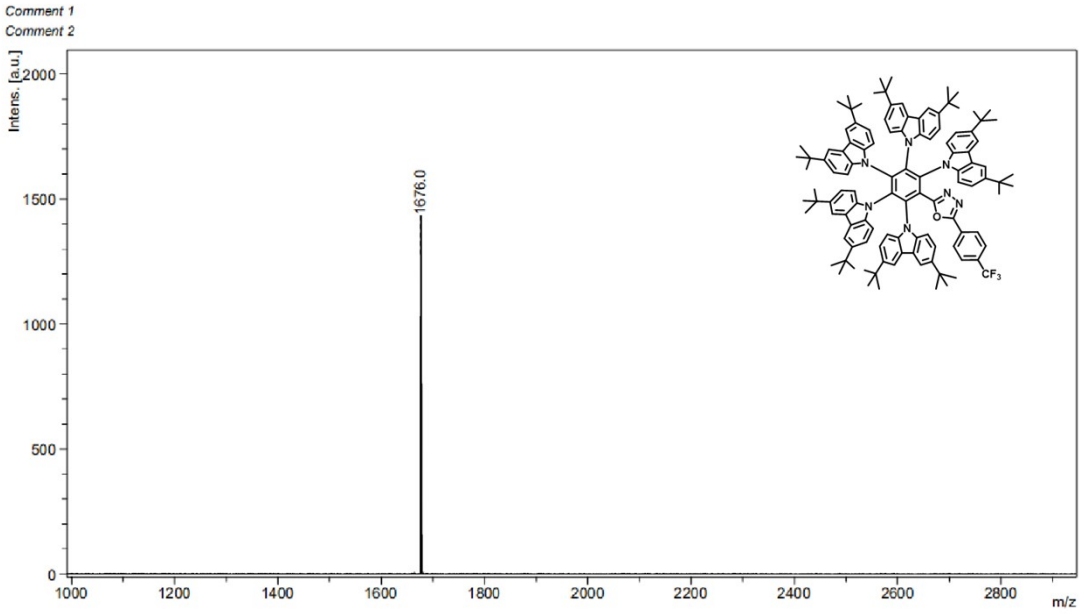

Fig. S4. ^{1}H NMR spectra, ^{13}C NMR spectra and mass spectrometry of the target compound *p*$CF_3$5tCzOXD.

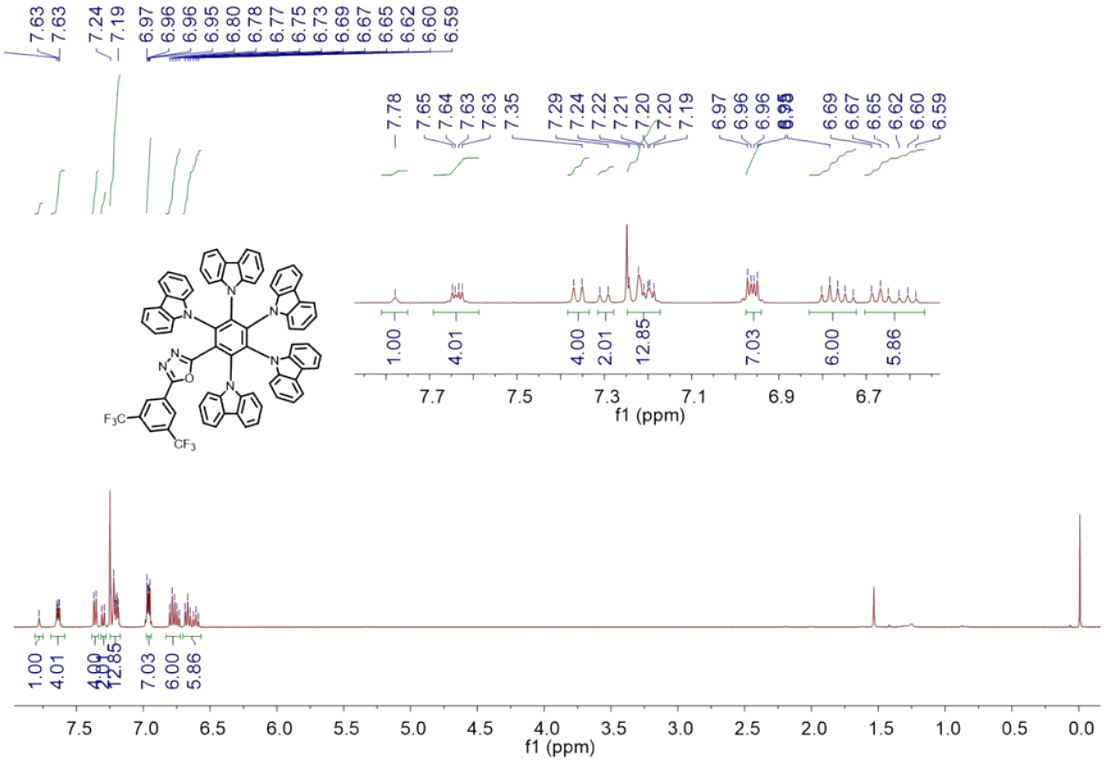

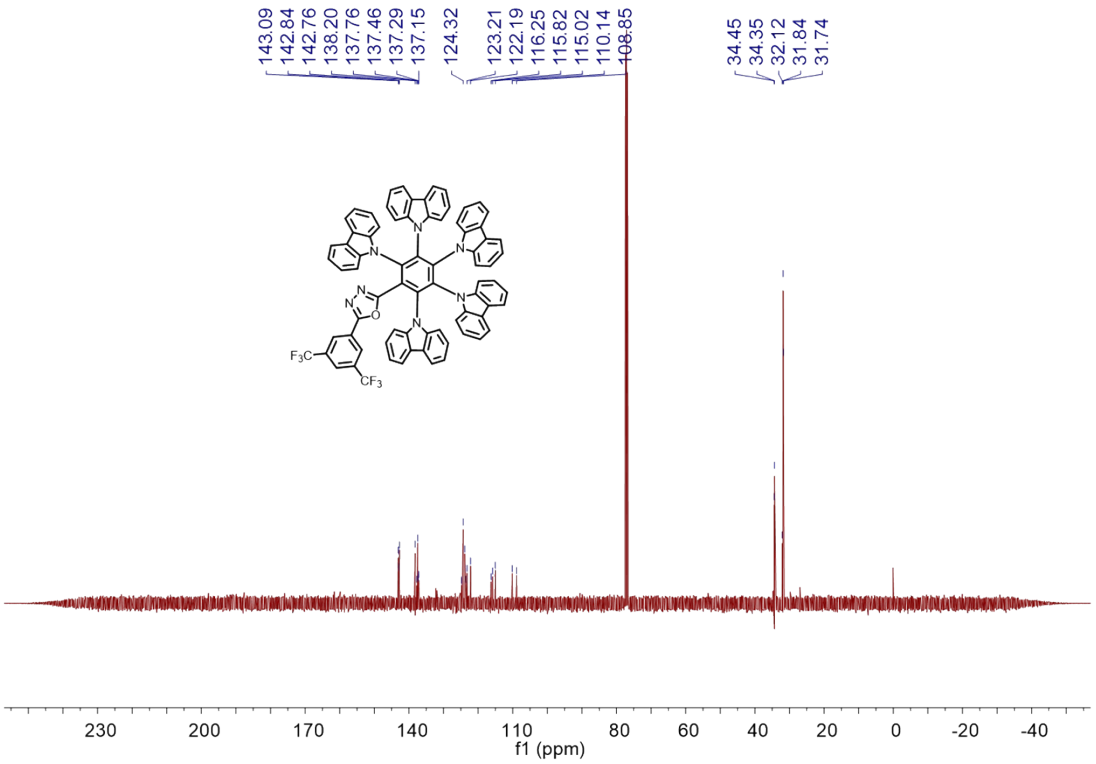

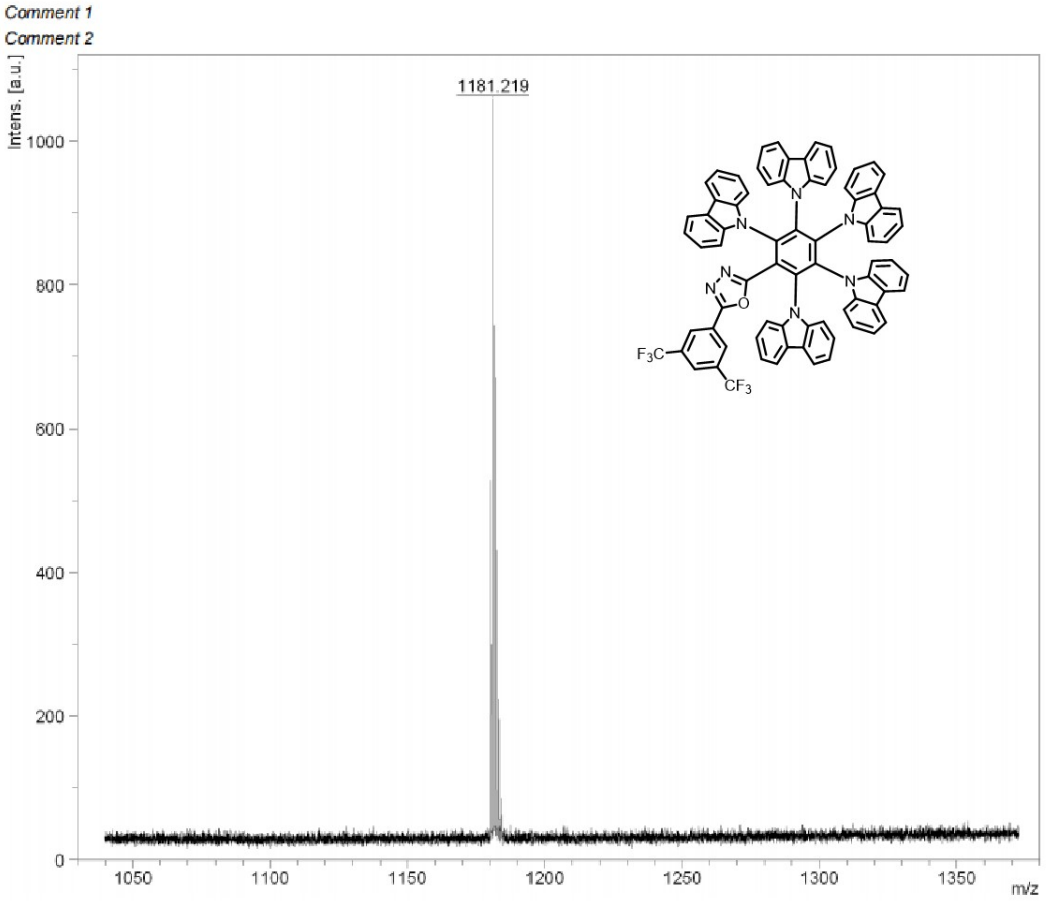

Fig. S5. ^{1}H NMR spectra, ^{13}C NMR spectra and mass spectrometry of the target compound $dCF_3$5CzOXD.

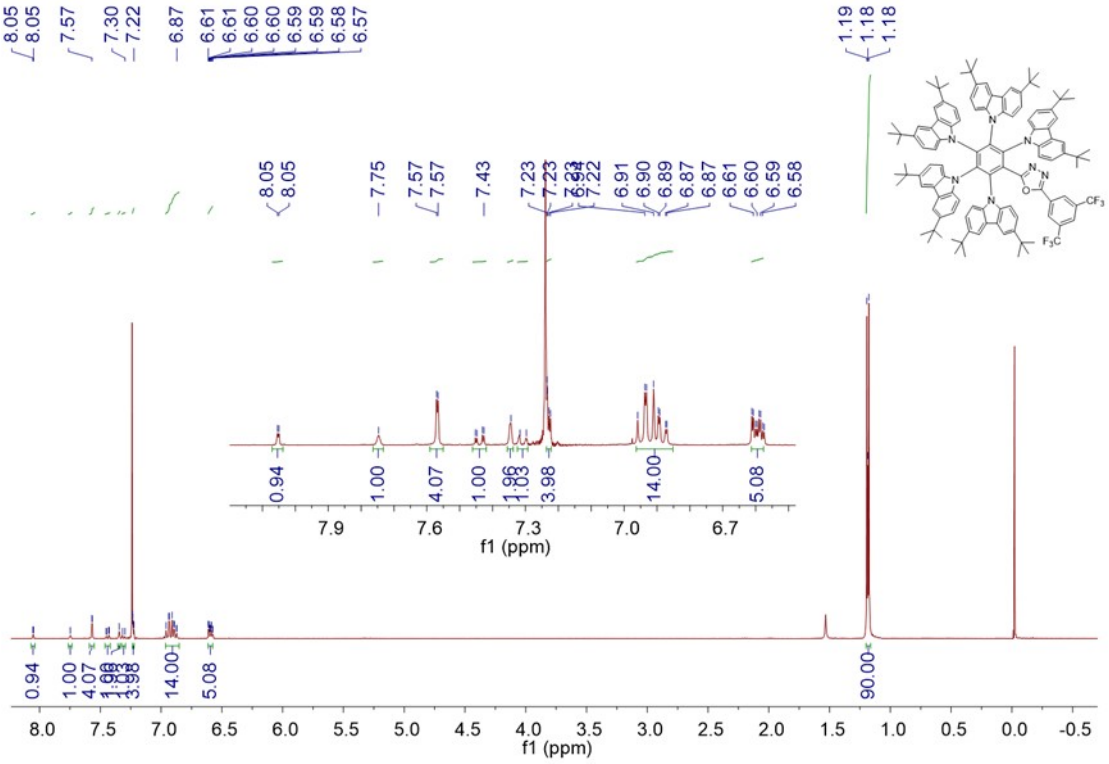
8.05
8.05
7.57
7.30
7.22
6.87
6.61
6.61
6.60
6.60
6.59
6.59
6.58
6.57
1.19
1.18
1.18
7.75
7.57
7.57
7.43
7.23
7.23
6.91
6.90
6.89
6.87
6.87
6.61
6.60
6.59
6.58
0.94
1.00
4.07
1.00
1.96
1.03
3.98
14.00
5.08
90.00
f1 (ppm)

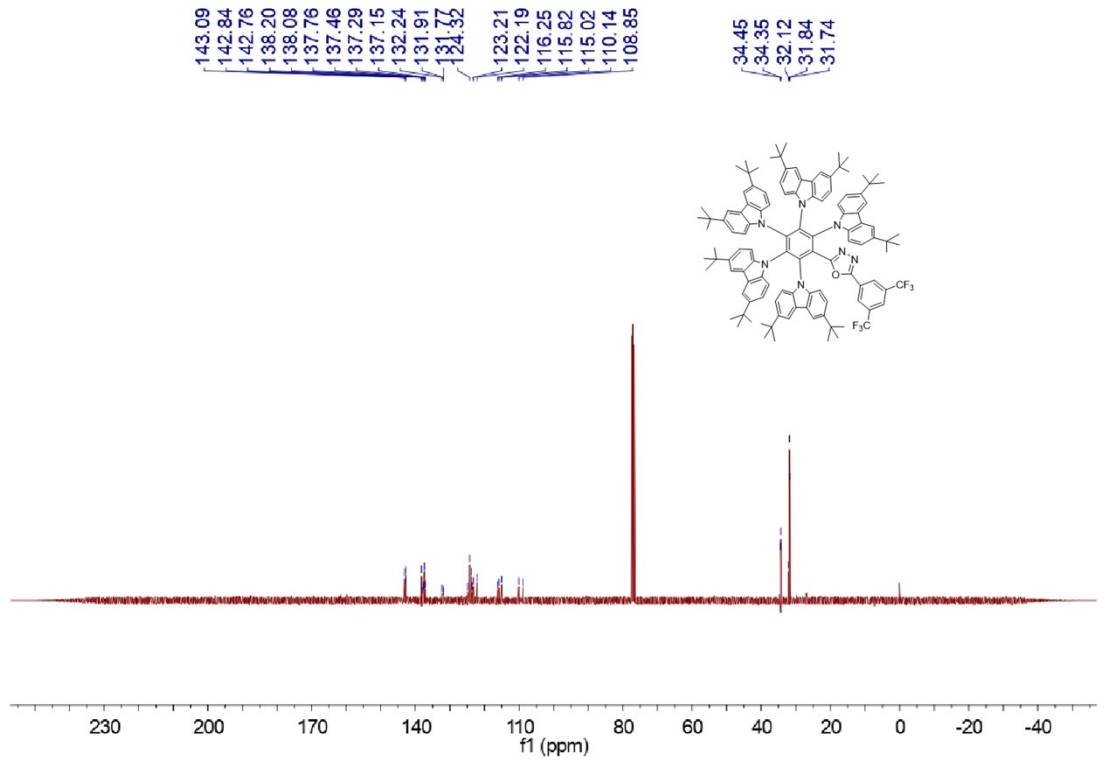
143.09
142.84
142.76
138.20
138.08
137.76
137.46
137.29
137.15
132.24
131.91
131.77
124.32
123.21
122.19
116.25
115.82
115.02
110.14
108.85
34.45
34.35
32.12
31.84
31.74
f1 (ppm)

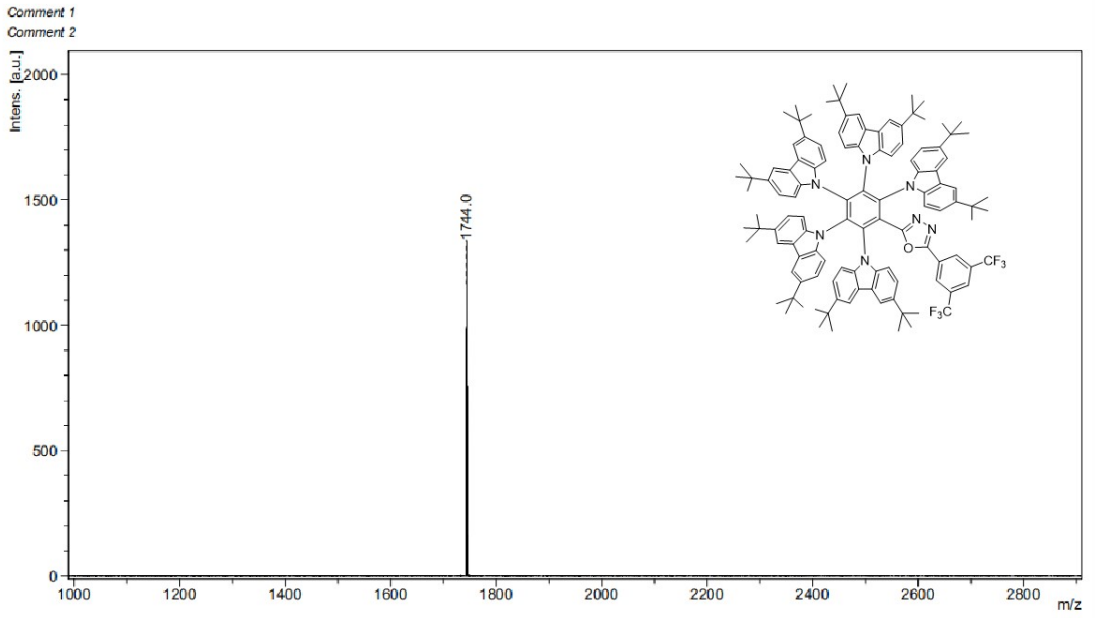

Fig. S6. ^{1}H NMR spectra, ^{13}C NMR spectra and mass spectrometry of the target compound dCF$_3$5tCzOXD.

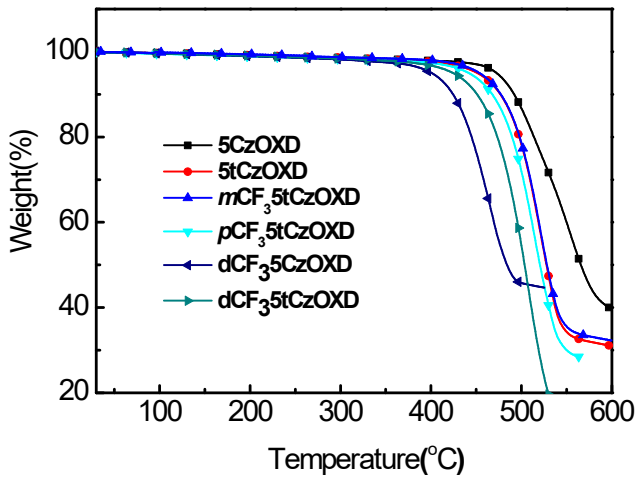

Fig. S7. TGA curves for compound 5CzOXD, 5tCzOXD, *m*CF$_3$5tCzOXD, *p*CF$_3$5tCzOXD, dCF$_3$5CzOXD and dCF$_3$5tCzOXD.

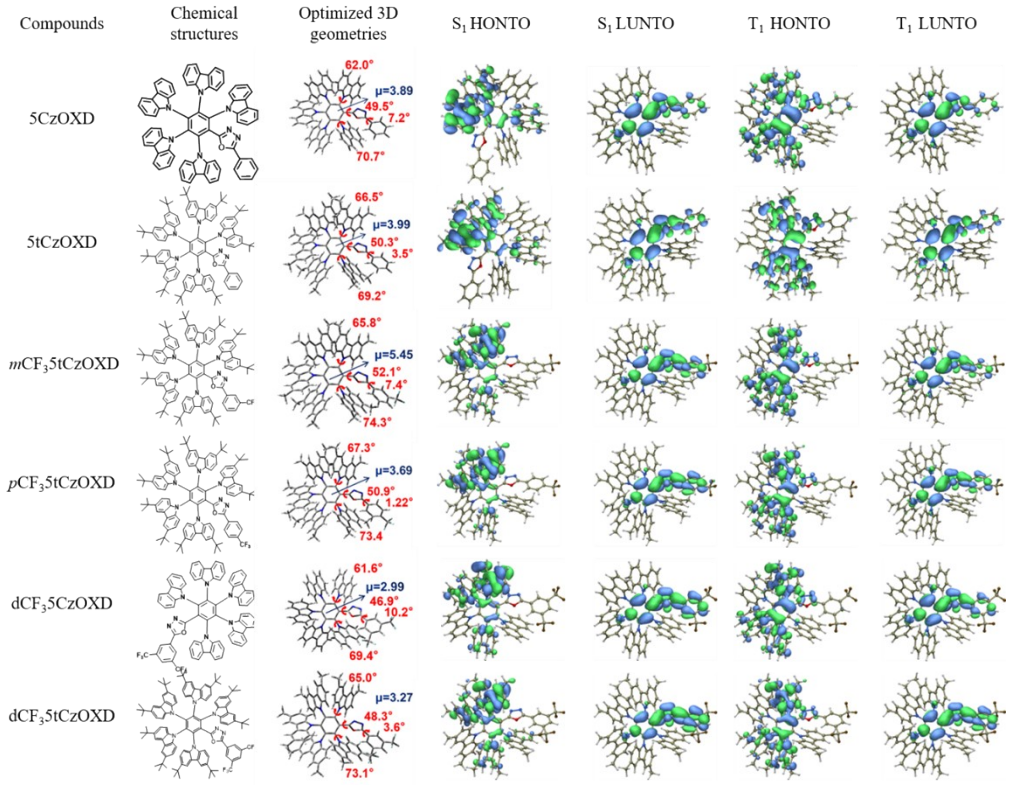

Fig S8. Chemical structures,optimized geometry, and highest occupied and lowest unoccupied natural transition orbitals of the lowest singlet (S_1) and triplet excited (T_1) states of the six compounds.

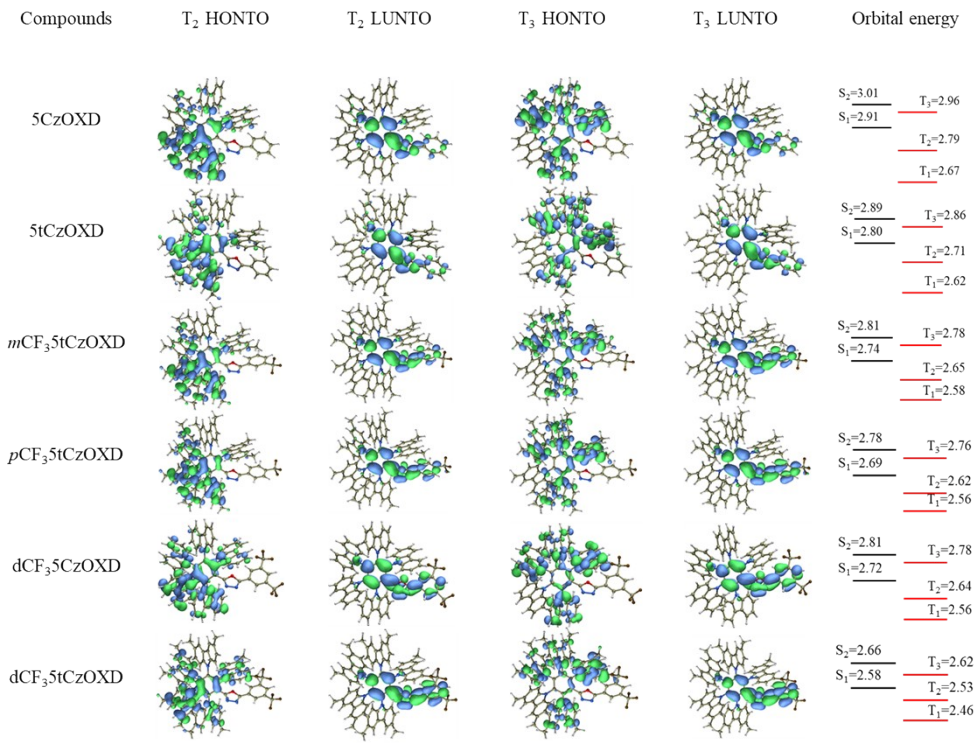

Fig S9. Highest occupied and lowest unoccupied natural transition orbitals of T_2 and T_3 states and the calculated energy levels of the six compounds.

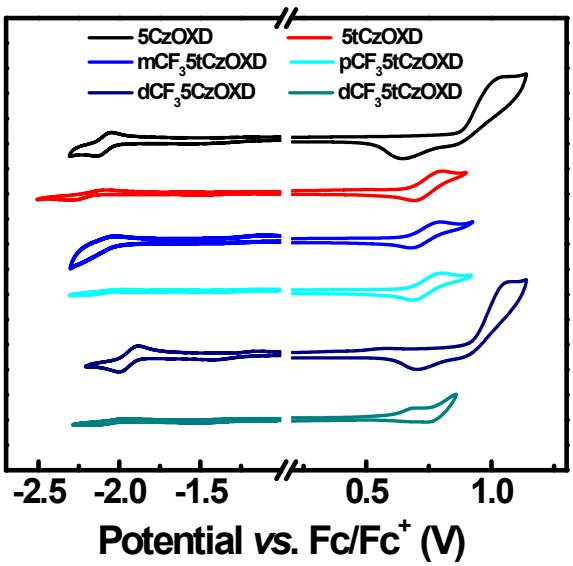

Fig. S10. Cyclic voltammograms of compound 5CzOXD, 5tCzOXD, *m*$CF_3$5tCzOXD, *p*$CF_3$5tCzOXD, d$CF_3$5CzOXD and d$CF_3$5tCzOXD in CH_2Cl_2 for oxidation scan and DMF in reduction.

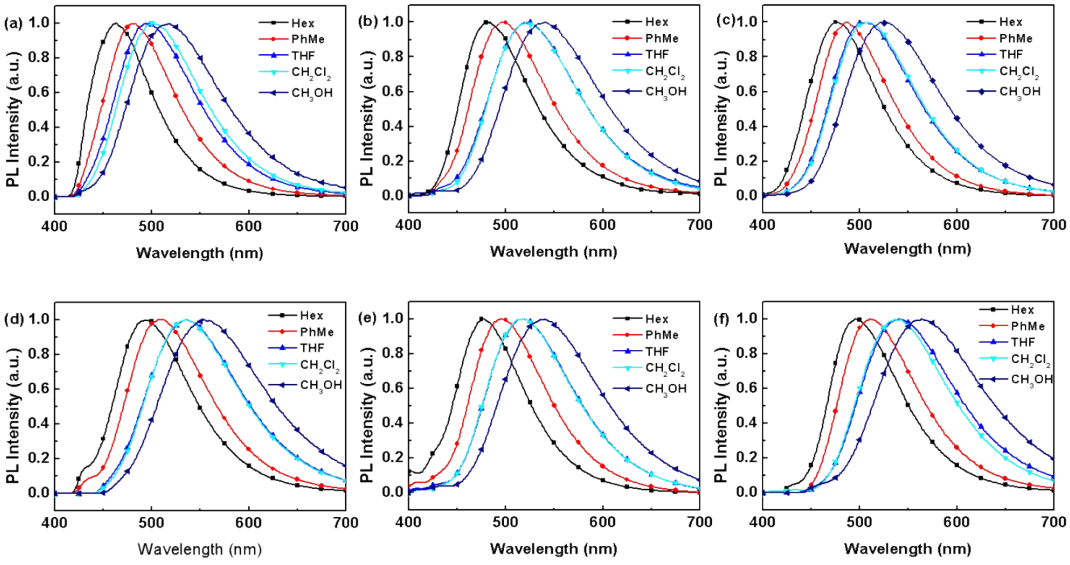

Fig. S11. PL spectra of 5CzOXD(a), 5tCzOXD(b), *m*$CF_3$5tCzOXD(c), *p*$CF_3$5tCzOXD(d), d$CF_3$5CzOXD(e) and d$CF_3$5tCzOXD(f) in various solvents at room temperature.

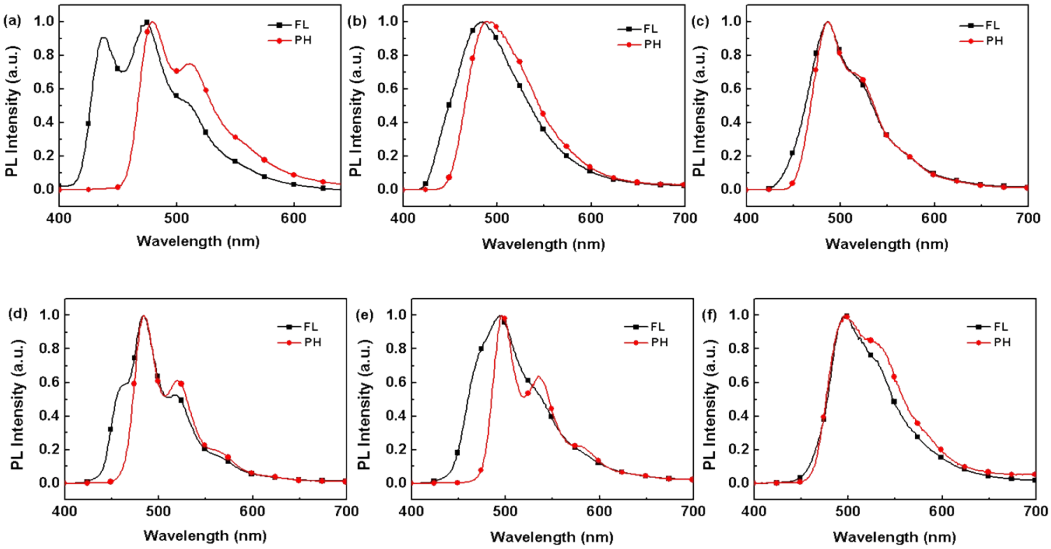

Fig. S12. Normalized fluorescence and phosphorescence spectra of 5CzOXD(a), 5tCzOXD(b), *m*$CF_3$5tCzOXD(c), *p*$CF_3$5tCzOXD(d), d$CF_3$5CzOXD(e) and d$CF_3$5tCzOXD(f) in neat films at 77 K.

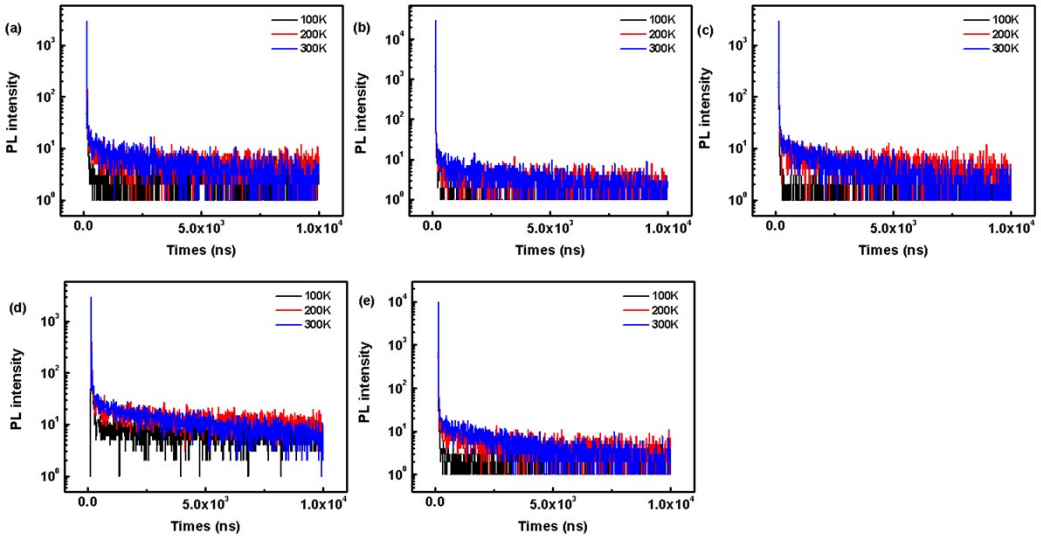

Fig. S13. Transient PL decay curves of 5tCzOXD(a), *m*$CF_3$5tCzOXD(b), *p*$CF_3$5tCzOXD(c), d$CF_3$5CzOXD(d) and d$CF_3$5tCzOXD(e) measured at 100-300 K.

Table S1. Summary of the PLQY of 5CzOXD and $dCF_3$5tCzOXD in *o*-CzOXD films at different doping concentration.

Compounds	Concentration [wt%]	Φ_{PLQY} [%]
5CzOXD	10	25.3
	20	26.8
	30	36.8
	40	42.1
	50	38.9
	100	9
$dCF_3$5tCzOXD	10	87.8
	20	71.2
	30	57.9
	40	52.7
	50	44.0
	100	18

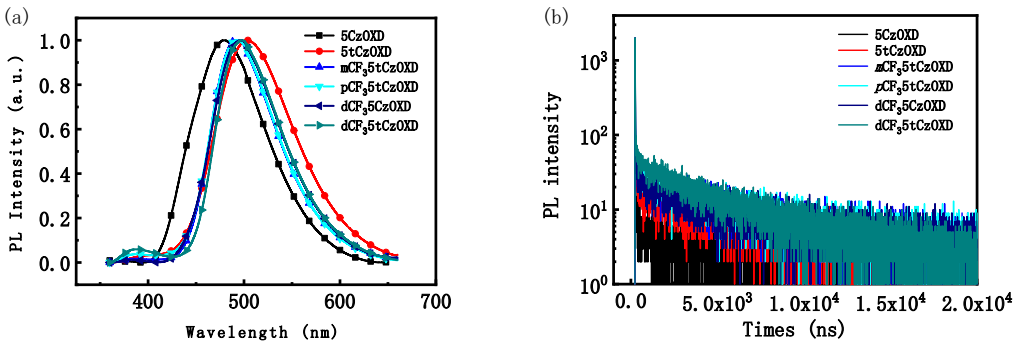

Fig S14. (a) Normalized PL spectra and (b) transient PL decay curves of six emitters in 26DCzPPy host at 10% doping concentration.

Table S2. Summary of the physical properties of the compounds in 26DCzPPy films.

Compounds	5CzOXD	5tCzOXD	*m*$CF_3$5tCzOXD	*p*$CF_3$5tCzOXD	$dCF_3$5CzOXD	$dCF_3$5tCzOXD
λ_{em} [nm]	479	503	491	491	496	497
τ_1 [ns]	6.3	5.4	6.2	6.2	9.0	7.0
τ_2 [ns]	1104	4112	4352	4176	4383	3864
Φ_{PLQY} [%]	14.2	29.5	49.4	36.3	34.5	54.0

References

1 A. D. Becke, *Phys. Rev. A*, 1988; **38**, 3098.

2 C. Lee, W. Yang, and R. G. Parr, *Phys. Rev. B*, 1988, **37**, 785.

3 J.-X. Chen, K. Wang, C.-J. Zheng, M. Zhang, Y.-Z. Shi, S.-L. Tao, H. Lin, W. Liu, W.-W. Tao, X.-M. Ou and X.-H. Zhang, *Adv. Sci.*, 2018, **5**, 1800436.

4 K.-C. Pan, S.-W. Li, Y.-Y. Ho, Y.-J. Shiu, W.-L. Tsai, M. Jiao, W.-K. Lee, C.-C. Wu, C.-L. Chung, T. Chatterjee, Y.-S. Li, L.-T. Wong, H.-C. Hu, C.-C. Chen, M.-T. Lee, *Adv. Funct. Mater.*, 2016, **26**,7560.